Chinese Chemical Letters 37 (2026) 111829

Contents lists available at ScienceDirect

Chinese Chemical Letters

journal homepage: www.elsevier.com/locate/cclet

Exploring the composition space of quinary metal oxides for oxygen evolution reaction on an automated platform

Zhongyin Zhao[a,b], Yunfan Fu[c], Sihui Chen[c], Zhenye Liang[b], Shaoru Cheng[c], Xueshan Hu[b], Yunchao Yin[a], Jinlong Yang[a,*], Yang Liu[d,*], Jiayu Wan[b,*]

[a] Guangdong Provincial Key Laboratory of New Energy Materials Service Safety, Shenzhen Key Laboratory of Energy Electrocatalytic Materials, College of Materials Science and Engineering, College of Physics and Optoelectronic Engineering, Shenzhen University, Shenzhen 518060, China
[b] Future Battery Research Center, Global Institute of Future Technology, Shanghai Jiaotong University, Shanghai 200240, China
[c] Department of Mechanical and Energy Engineering, Southern University of Science and Technology, Shenzhen 518055, China
[d] Data Science Research Center, Duke Kunshan University, Kunshan 215316, China

ARTICLE INFO

Article history:
Received 7 July 2025
Revised 6 September 2025
Accepted 11 September 2025
Available online 12 September 2025

Keywords:
Machine learning
Electrocatalysts
Automation
Oxygen evolution reaction
Transition metal oxides

ABSTRACT

The oxygen evolution reaction (OER) is crucial for renewable energy systems, such as water splitting and metal air batteries. However, the slow kinetics of OER significantly limits the overall energy conversion efficiency, necessitating effective catalysts. The multielement transition metal oxides offer a promising alternative compared to precious metal oxides, yet their composition optimization remains challenging due to the vastness of the combinatorial space. Traditional trial-and-error approaches are labor-intensive and inefficient. To address this challenge, we develop an innovative automated platform integrating machine learning (ML) with Bayesian optimization for rapid and cost-effective synthesis and evaluation of electrocatalysts. This platform allows the automation of the entire experimental process, from synthesis to evaluation, enabling real-time feedback and guiding subsequent experiments. In a continuous operation of 32 h, the platform conducted 96 experiments to optimize the composition of (Ni-Fe-Co-Mn-Mo)O_x, resulting in an electrocatalyst with an overpotential of 231 mV at 10 mA/cm^2. This automated approach significantly reduces manual intervention and enhances efficiency, proving to be a valuable tool for optimizing materials in complex, multidimensional spaces.

© 2026 Published by Elsevier B.V. on behalf of Chinese Chemical Society and Institute of Materia Medica, Chinese Academy of Medical Sciences.

The oxygen evolution reaction (OER) as a half-reaction has a paramount role in electrocatalytic water splitting, rechargeable Zn-air batteries (ZAB) and electrocatalytic CO_2/N_2 reduction [1–6]. However, the OER process is governed by multistep four-electron transfer, which leads to very slow kinetic reaction that often require catalysts to increase their reaction rate [7,8]. Currently, precious metal oxides (*e.g.*, RuO_2/IrO_2) are the most effective electrocatalysts for OER, but their high price and scarcity preclude scalable applications [9]. Therefore, it is of great necessity to develop active, cost-effective and earth-abundant OER electrocatalysts [10,11].

Transition metal oxides have been verified as one of the most promising cost-effective OER electrocatalysts to replace their noble metal counterparts [12]. In order to further improve their activity, multiple metal elements mixing is considered as an effective strategy, which can modulate the electronic structure and optimize the adsorption energy of active sites during the OER process [13,14]. However, when more than three metal elements are introduced, the combinatorial possibilities are too large, which makes it a time-consuming and labor-intensive process to investigate the influence of composition on the OER performance of the electrocatalyst by traditional trial-error method.

Although high-throughput methodologies enable large-scale exploration of the vast compositional space of mixed-metal oxides, their synthesis and evaluation remain time-consuming [15–18]. Additionally, in conventional high-throughput experimentation, processes are typically conducted in batches without an integrated feedback mechanism in between, leading to inefficiencies and unnecessary consumption of time and resources. Very recently, many studies have demonstrated that the automated experiments integrate with machine learning (ML) are efficient in materials research [19–24]. For example, Ceder *et al.* have employed an

* Corresponding authors.
E-mail addresses: yangjl18@szu.edu.cn (J. Yang), yang.liu2@dukekunshan.edu.cn (Y. Liu), wanjy@sjtu.edu.cn (J. Wan).

https://doi.org/10.1016/j.cclet.2025.111829
1001-8417/© 2026 Published by Elsevier B.V. on behalf of Chinese Chemical Society and Institute of Materia Medica, Chinese Academy of Medical Sciences.

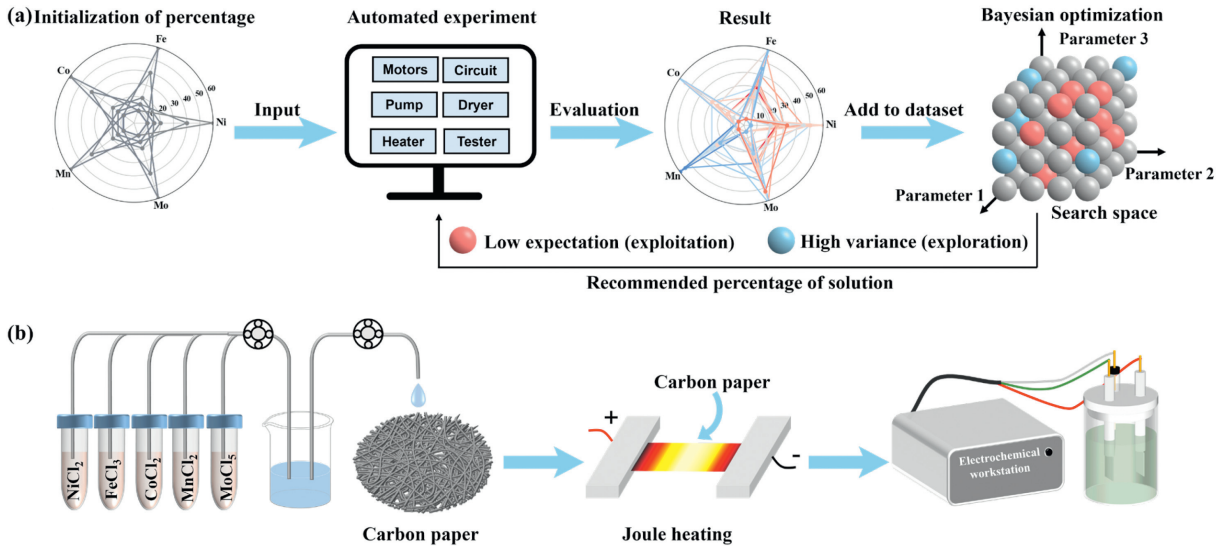


Fig. 1. (a) Schematic diagram of automated platform for synthesizing electrocatalysts. (b) The diagram of the components in the platform for (Ni-Fe-Co-Mn-Mo)O_x electrocatalysts.

autonomous laboratory to synthesize 41 new compounds in 17 days of continuous with a 71 % success rate [19]. Cooper *et al.* have developed a mobile robot to realize experimental operations and completed 688 experiments on improving activity of photocatalysts within an experimental space of 10 variables, greatly increasing the efficiency of the experiments [21]. However, the high cost of automated and robotic equipment makes fully automated or autonomous experimentation a luxury. Additionally, the conventional synthesis of these materials is time-consuming, further hindering the discovery process. These limitations contribute to the inaccessibility of automated platforms for most standard research laboratories.

In this paper, we present an efficient and cost-effective automated platform that integrates ML based on Bayesian optimization, automated ultrafast synthesis and automated evaluation to optimize the composition of (Ni-Fe-Co-Mn-Mo)O_x for enhanced electrocatalytic activity. Leveraging automated ultrafast synthesis in milliseconds [25–27] and real-time feedback from each evaluation, this platform effectively guides subsequent experiments, significantly reducing the total number required. Over 32 h of continuous operation, the platform completed 96 experiments and identified an optimized composition of (Ni-Fe-Co-Mn-Mo)O_x for improved OER activity. We envision this platform as a key step towards autonomous discovery of advanced materials, accelerating progress in renewable energy technologies.

The schematic representation of the automated platform for synthesizing electrocatalysts is illustrated in Fig. 1a. Initially, we conducted experiments to build a database comprising of random samples with varying compositions, along with their corresponding OER performance, which served as input for training and understanding the composition-performance relationship. Guided by this database and the latest result *via* the Bayesian optimization, subsequent experiments were iteratively performed using automated synthesis and testing of the samples, continuing until no further significant improvement in performance is observed. Notably, in our experimental design, the materials are synthesized and evaluated individually rather than in batches, allowing for prompt evaluation of electrocatalytic activity following synthesis. This unified synthesis and evaluation approach not only furnishes timely feedback on experimental outcomes but also streamlines the search for the optimal parameter set guided by the algorithm, avoiding exhaustive iteration through the entire library (Fig. S1 in Supporting information). To validate this hypothesis, quinary metal oxides (Ni-Fe-Co-Mn-Mo)O_x were selected as model electrocatalysts and their OER performance were investigated. To overcome the challenge of prolonged calcination in oxide preparation, we employed an ultrafast synthesis approach using a joule-heating device integrated into the automated platform for rapid, automated synthesis of metal oxides. The overpotentials were measured through linear sweep voltammetry to quantify their OER activity.

The diagram illustrating the platform for the synthesizing and evaluating (Ni-Fe-Co-Mn-Mo)O_x electrocatalysts is depicted schematically in Fig. 1b. The platform consisted of a materials synthesis unit, which included precursor mixing and ultrafast joule-heating synthesis, an electrochemical testing unit that comprised an electrochemical workstation and automated testing, and an intelligent control and optimization unit. The system occupies a compact footprint of just 120 cm × 60 cm with a cost of less than $6000 (Table S1 in Supporting information). A typical material preparation and testing process includes solution preparation, sample deposition, and electrochemical testing. Currently, the solution preparation module was equipped with 12 channels, though only six were used in the experiments. These channels draw preconfigured solutions (0.05 mol/L $NiCl_2$, 0.05 mol/L $CoCl_2$, 0.05 mol/L $FeCl_3$, 0.05 mol/L $MnCl_2$ and 0.05 mol/L $MoCl_5$, with ethanol as solvent) from the repository and blend them to achieve the desired elemental ratios. Custom-built syringe pumps, known for their high precision, were used to dispense the solutions. The (Ni-Fe-Co-Mn-Mo)O_x was synthesized on carbon paper by first depositing the precursor solution onto the paper and dried with mild heating. Joule heating is then applied through the carbon paper to achieve the desired (Ni-Fe-Co-Mn-Mo)O_x material. The carbon paper sample was subsequently transferred between modules using a system of linear motors and programmed clamps. While most operations are automated, manual intervention is still required for tasks such as replacing carbon paper, preparing and replenishing solution.

At the beginning of the automatic experiment, the carbon paper was firstly removed from the carbon paper rack and positioned using a programmed linear motor and clamp. The pump automatically withdrew and mixed the solution (total volume of 40 μL) based on the input elemental ratios before dropping the so-

(a)

Parameters in Automated Experiment

Device	#	Parameter	Value
Pump	1	Solution percentage	Data to be input
	2	Chloride solution	[Total] = 0.05 M
	3	Drop volume	40 μL
	4	Flushing time	100 s
Dryer	5	Temperature	60 °C
	6	Drying time	10 min
Heater	7	Voltage	30 V
	8	Current	1.2 A
	9	Heating time	100 ms
Tester	10	Electrolyte	[KOH] = 1 M
	11	CV	0/0.8/0 V @ 0.1 V/s X 20
	12	LSV	0/0.8 V @ 0.005 V/s

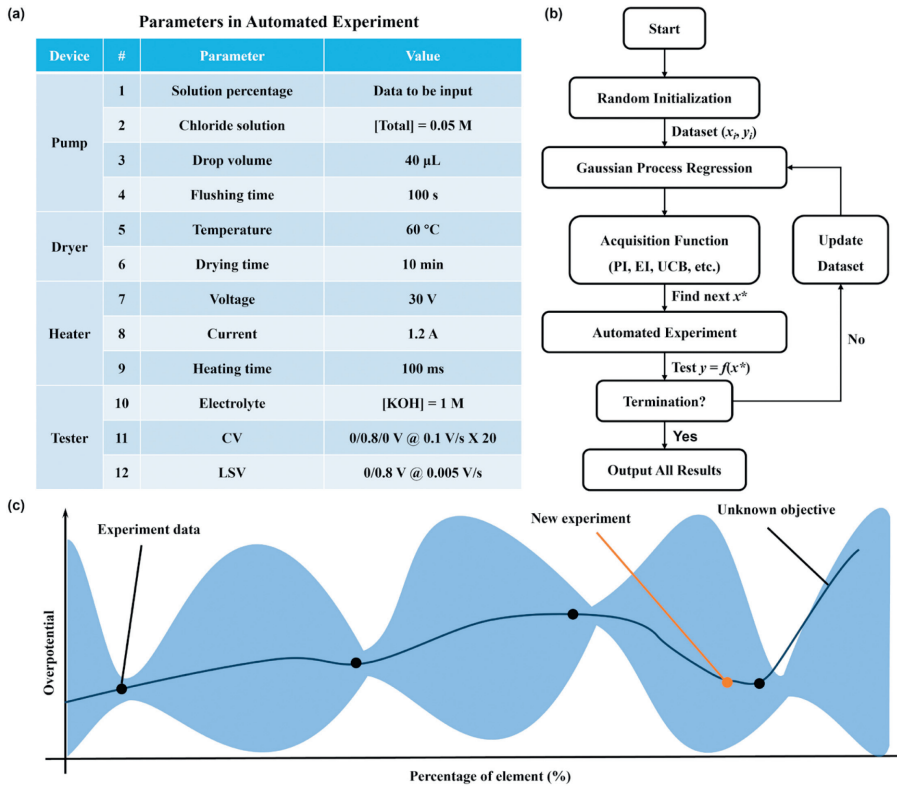


Fig. 2. (a) A sequence of steps and parameters with steps in automated experiment. (b) Workflow of the Bayesian optimization algorithm. (c) Graphical overview of Bayesian optimization.

lution onto the carbon paper in predetermined quantities and intervals. Following each individual experiment, the mixing vessel were automatically emptied and flushed clean. The carbon paper laden with the mixed solution was then subjected to drying under an infrared lamp for 10 min to eliminate ethanol and transported by linear motors to a joule heating module for rapid heating of 100 ms. Upon completion of electrocatalyst synthesis, the OER performance test is performed in 1 mol/L KOH in three-electrode system at 5 mV/s, in which carbon paper loaded with electrocatalysts was utilized as a working electrode, Hg/HgO electrode as the reference electrode and a graphite rod as the counter electrode.

To execute a single experiment, the main control program was developed using the Python programming language and utilized for controlling the Arduino demo board, syringe pump, and electrochemical workstation *via* serial communication. Simultaneously, the Arduino demo board served as the lower-tier controller for managing motor movements and relay switches. Steps designed for this work are shown in Fig. 2a. While these steps were remained consistent for individual experiment, numerical parameters including solution concentration, volume, joule heating parameters, electrochemical parameters and time could be systematically adjusted and evaluated in closed-loop optimization. On the automation platform, the average duration for completing an individual experiment, including electrocatalyst preparation and performance testing, was approximately 20 min. Therefore, the combinatorial experiments containing these 96 different parameter sets can be run and completed in 32 h.

The Bayesian optimization algorithm is a global optimization technique capable of efficiently finding the global optimum of any function within a search space, thereby reducing the total number of required experiments (Fig. 2b). To explore and optimize the composition of the (Ni-Fe-Co-Mn-Mo)O_x electrocatalysts for OER, 36 samples with varying component compositions and corresponding overpotentials were selected as starting point for the Bayesian optimization, whereof 31 samples were selected randomly and 5 samples were “extreme” composition that consisted of 80 % of one element and 5 % of each of remaining element (Table S2 in Supporting information). A well-defined output parameter for OER activity during the optimization process was established as the overpotential at a current density of 10 mA/cm^2. A Gaussian process regressor (GPR) model simulated the complex relationship between overpotential and element ratios of electrocatalysts was then constructed based on the experimental results of the initial samples, where the overpotential $f(x)$ corresponding to an element ratio x is treated as a random variable with a joint multivariate Gaussian distribution. Using inferences from known data points (x_i,y_i), we can compute the mean value $\mu(x^*)$ and uncertainty $\sigma^2(x^*)$ for each unknown data point by the following Eqs. 1 and 2.

$$\mu(x^*) = k(x^*, x_i)\left(K + \sigma^2{}_n I\right)^{-1} y_i \tag{1}$$

$$\sigma^2(x^*) = k(x^*, x^*) - k(x^*, x_i)\left(K + \sigma^2{}_n I\right)^{-1} k(x^*, x_i) \tag{2}$$

As shown in Fig. 2c, black points represent the actual data points, and the Gaussian process regressor constructs a mathematical model based on these points. The black line denotes the predicted values for each point in the search space, while the blue shaded area indicates prediction uncertainty. In the vertical direction, a larger light blue shaded area indicates greater prediction uncertainty. Additionally, the Probability of Improvement (PI) acquisition function (Eq. 3) is used to measure the potential benefit of selecting an unsearched point under the current Gaussian process regressor model,

$$PI(x) = P[f(x) \le f\left(x^-\right) - \xi] = \Phi\left[\left(f\left(x^-\right) - \mu(x) - \xi\right)/\sigma(x)\right] \tag{3}$$

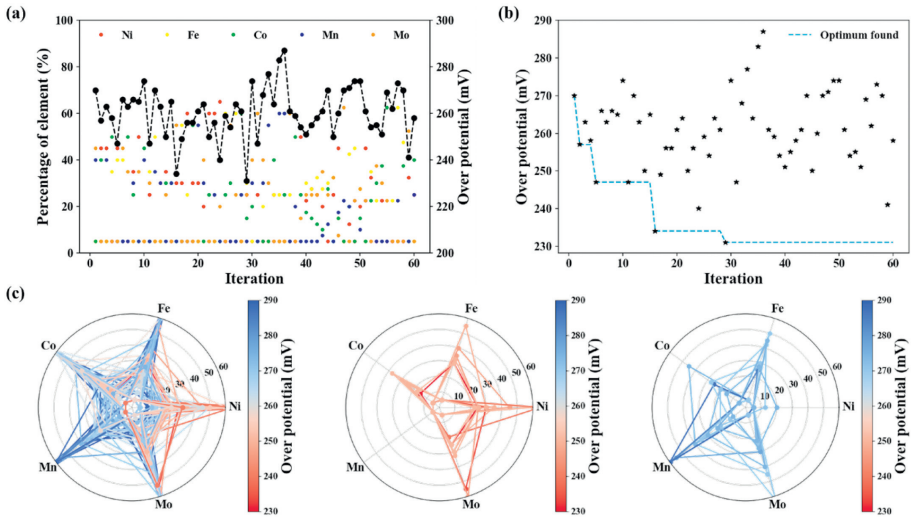


Fig. 3. (a) The compositional ratios and overpotential of (Ni-Fe-Co-Mn-Mo)O_x electrocatalysts in every Bayesian optimization round. (b) Learning rate during this optimization. (c) Radar plot showing the relationship between overpotential and components.

where $f(x^-)$ represents the lowest overpotential value among the known data points, and ξ is a parameter controlling the exploration degree. A smaller ξ values emphasize exploiting known information, whereas a larger ξ values stress exploring unexplored regions. In each iteration, the point that maximizes *PI* (Eq. 4) is selected as the input for the next iteration to increase the probability of obtaining a lower overpotential than the currently known minimum.

$$x_{\text{next}} = argmax_x PI(x) \tag{4}$$

As the iterations increased, the automated experimental platform automatically conducted the experiment in accordance with Bayesian optimization guidelines. The collected data continuously enriched the dataset, enhancing the accuracy of the GPR model and providing a reliable guide for subsequent experiment steps. This closed-loop optimization strategy could be continued until a user-set termination condition was achieved.

Fig. 3a presents the results of the automated experiment using closed-loop optimization guided by Bayesian optimization. Each optimization cycle proposed a compositional ratio of various metal elements aimed at minimizing overpotential. In the 29th iteration, the electrocatalyst with the lowest overpotential was identified with a compositional ratio of Ni:Fe:Co:Mn:Mo was 25:30:15:5:25, achieving an overpotential of 231 mV at 10 mA/cm^2. Moreover, ($Ni_{25}Fe_{30}Co_{15}Mn_5Mo_{25}$)$O_x$ exhibited a long-term stability with negligible decay even after 60 h continuous operation (Fig. S2 in Supporting information). The learning rate during the Bayesian optimization was depicted in Fig. 3b Guided by Bayesian optimization, the experiments identified metal element proportions with lower overpotentials than all previous experiments at the 1st, 2nd, 5th, 16th and 29th iterations, respectively. However, beyond the 30th iterations, no additional metal element proportions with lower overpotential were found. Therefore, the experiment was terminated after the 60th iteration. It was noteworthy that only less than 0.2 % of all possible compositions (96 from 46,376) were experimentally explore to achieve the optimum level, strongly demonstrating the efficiency of our approach. Additionally, the radar plot revealed that an appropriate Ni content facilitated the reduction of overpotential, whereas an excessive Mn content was detrimental to its reduction. (Fig. 3c).

Furthermore, the LSV curves and corresponding Tafel slopes obtained from automated platform were compared with those from manual testing (Figs. 4a-f and Fig. S3 in Supporting information). While there were some discrepancies in overpotentials and Tafel slopes, the overall trends in OER performance remained consistent, demonstrating the reliability and accuracy of our approach. This outstanding OER performance of ($Ni_{25}Fe_{30}Co_{15}Mn_5Mo_{25}$)$O_x$ make it superior to the recently reported highly active electrocatalysts in alkaline media (Fig. 4g) [28–40]. To verify the successful synthesis of ($Ni_{25}Fe_{30}Co_{15}Mn5Mo_{25}$)$O_x$ particles *via* the automated experimental platform, the morphologies of ($Ni_{25}Fe_{30}Co_{15}Mn_5Mo_{25}$)$O_x$ were characterized by transmission microscopy (TEM). Figs. 4h-j showed ($Ni_{25}Fe_{30}Co_{15}Mn_5Mo_{25}$)$O_x$ nanoparticles were uniformly grown on carbon paper with a diameter of about 50 nm. To further study the structure of ($Ni_{25}Fe_{30}Co_{15}Mn_5Mo_{25}$)$O_x$ nanoparticles, high-resolution TEM (HRTEM) was carried out. Typical lattice spacing of 0.29 nm and 0.25 nm was indexed to the (220) plane and (311) plane of spinel of ($Ni_{25}Fe_{30}Co_{15}Mn_5Mo_{25}$)$O_x$ nanoparticles (JCPDS No. 71–0852) (Fig. 4k). The corresponding selected electron diffraction (SAED) further demonstrated the as prepared ($Ni_{25}Fe_{30}Co_{15}Mn_5Mo_{25}$)$O_x$ nanoparticles have a cubic spinel structure (Fig. 4k, inset). The high-angle annular dark-field scanning transmission electron microscopy (HAADF-STEM) and X-ray energy dispersive spectroscopy (EDS) mapping confirmed the homogenous of Ni, Fe, Co, Mn and Mo in ($Ni_{25}Fe_{30}Co_{15}Mn_5Mo_{25}$)$O_x$ nanoparticles and the molar ratio of Ni, Fe, Co, Mn and Mo was closed to the feed ratios in the precursor solution (Fig. 4l and Table S3 in Supporting information).

In summary, we developed an innovative and cost-effective automated platform that integrated ML, automated synthesis and real-time evaluation to accelerate the development of electrocatalysts for OER. This approach, exemplified by the optimization of multielement (Ni-Fe-Co-Mn-Mo)O_x electrocatalysts, significantly reduces manual intervention and speeds the discovery of highly efficient catalysts. By conducting 96 experiments over 32 h, the platform identified an optimal composition of (Ni-Fe-Co-Mn-Mo)O_x with an overpotential of 231 mV at 10 mA/cm^2, highlighting its effectiveness in exploring complex compositional spaces. The platform not only streamlines the experimental process but also provides real-time feedback during the search of optimal parameters, enabling rapid and informed decision-making. Its cost-efficiency and adaptability make it an attractive solution for future research, enhancing accessibility to laboratories. This automated platform can be further expanded to optimize other material systems, potentially revolutionizing materials development across various renewable energy applications and beyond.

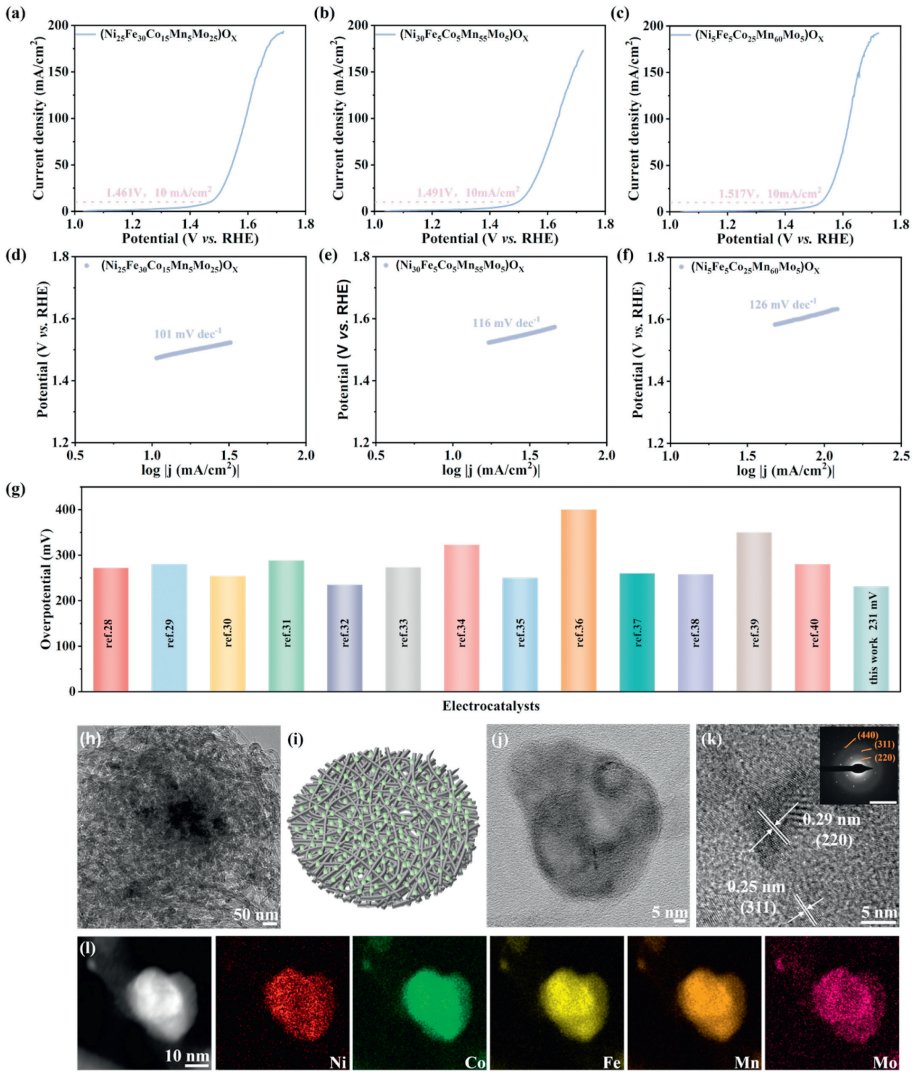


Fig. 4. The LSV curves of (a) $(Ni_{25}Fe_{30}Co_{15}Mn_5Mo_{25})O_x$, (b) $(Ni_{30}Fe_5Co_5Mn_{55}Mo_5)O_x$ and (c) $(Ni_5Fe_5Co_{25}Mn_{60}Mo_5)O_x$ and their corresponding Tafel slopes of (d) $(Ni_{25}Fe_{30}Co_{15}Mn_5Mo_{25})O_x$, (e) $(Ni_{30}Fe_5Co_5Mn_{55}Mo_5)O_x$ and (f) $(Ni_5Fe_5Co_{25}Mn_{60}Mo_5)O_x$ obtained from automated platform. (g) Comparison of the catalytic OER performance between $(Ni_{25}Fe_{30}Co_{15}Mn_5Mo_{25})O_x$ and the electrocatalysts reported in recent literature in alkaline media. (h) TEM image and (i) schematic diagram of $(Ni_{25}Fe_{30}Co_{15}Mn_5Mo_{25})O_x$ nanoparticles grown on carbon paper. (j) TEM image of $(Ni_{25}Fe_{30}Co_{15}Mn_5Mo_{25})O_x$ nanoparticles scratched off from carbon paper. (k) HRTEM image of $(Ni_{25}Fe_{30}Co_{15}Mn_5Mo_{25})O_x$ nanoparticles. The inset shows the SAED pattern of $(Ni_{25}Fe_{30}Co_{15}Mn_5Mo_{25})O_x$ nanoparticles. (l) HAADF-STEM image and its corresponding EDS elemental mapping images of $(Ni_{25}Fe_{30}Co_{15}Mn_5Mo_{25})O_x$ nanoparticles.

Declaration of competing interest

The authors declare that they have no known competing financial interests or personal relationships that could have appeared to influence the work reported in this article.

CRediT authorship contribution statement

Zhongyin Zhao: Writing – review & editing, Writing – original draft, Visualization, Validation, Methodology, Investigation, Formal analysis, Data curation. **Yunfan Fu:** Software, Methodology, Investigation, Data curation. **Sihui Chen:** Visualization, Software, Data curation. **Zhenye Liang:** Visualization. **Shaoru Cheng:** Visualization, Methodology, Investigation. **Xueshan Hu:** Visualization. **Yunchao Yin:** Visualization. **Jinlong Yang:** Writing – review & editing, Supervision, Resources, Project administration, Funding acquisition. **Yang Liu:** Writing – review & editing, Supervision, Software, Project administration, Methodology. **Jiayu Wan:** Writing – review & editing, Supervision, Project administration, Methodology, Funding acquisition, Conceptualization.

Acknowledgments

This work was financially supported by the AI for Science Program (No. 2025-GZL-RGZN-BTBX-01012), Shanghai Municipal Commission of Economy and Informatization and Advanced Materials-National Science and Technology Major Project (No. 2024ZD0607400), the National Natural Science Foundation of China (No. 52172217), Guangdong Basic and Applied Basic Research Foundation (No. 2024B1515020031), and Shenzhen Science and Technology Program (Nos. 20231122113443001, ZDSYS20220527171401003). The authors also appreciate the Instrumental Analysis Center of Shenzhen University.

Supplementary materials

Supplementary material associated with this article can be found, in the online version, at doi:10.1016/j.cclet.2025.111829.

References

[1] F.T. Haase, A. Bergmann, T.E. Jones, et al., Nat. Energy 7 (2022) 765–773.

[2] Y. Sun, R. Li, X.X. Chen, et al., Adv. Energy Mater. 11 (2021) 2003755.
[3] T.P. Zhou, N. Zhang, C.Z. Wu, Y. Xie, Energy Envrion. Sci. 13 (2020) 1132–1153.
[4] Z.H. Chen, X.W. Peng, Z.X. Chen, et al., Adv. Mater. 35 (2023) 2209948.
[5] Y.M. Hao, Y.K. Kang, S.Y. Wang, et al., Angew. Chem. Int. Ed. 135 (2023) e202303200.
[6] D. Li, Y.Y. Qin, J. Liu, et al., Adv. Funct. Mater. 32 (2022) 2107056.
[7] L. Han, S. Dong, E. Wang, Adv. Mater. 28 (2016) 9266–9291.
[8] Y. Jiao, Y. Zheng, M. Jaroniec, S.Z. Qiao, Chem. Soc. Rev. 44 (2015) 2060–2086.
[9] G. Chen, Z.W. Hu, Y.P. Zhu, et al., Adv. Mater. 30 (2018) 1804333.
[10] B.H.R. Suryanto, Y. Wang, R.K. Hocking, W. Adamson, C. Zhao, Nat. Commun. 10 (2019) 5599.
[11] Z.Y. He, J. Zhang, Z.H. Gong, et al., Nat. Commun. 13 (2022) 2191.
[12] T.R. Cook, D.K. Dogutan, S.Y. Reece, et al., Chem. Rev. 110 (2010) 6474–6502.
[13] Y. Huang, L.W. Jiang, B.Y. Shi, K.M. Ryan, J.J. Wang, Adv. Sci. 8 (2021) 2101775.
[14] G.Q. Shen, R.R. Zhang, L. Pan, et al., Angew. Chem. Int. Ed. 59 (2020) 2313–2317.
[15] C.C. Yu, Q. Xiong, K. Yang, H.B. Chen, F. Pan, Adv. Mater. Technol. 6 (2021) 2001036.
[16] T. Zhang, Y.T. Wu, Y.H. Yu, et al., Appl. Surf. Sci. 588 (2022) 152959.
[17] A. Shinde, R.J.R. Jones, D. Guevarra, et al., Electrocatalysis 6 (2015) 229–236.
[18] J.A. Haber, Y. Cai, S.H. Jung, et al., Energy Environ. Sci. 7 (2014) 682–688.
[19] N.J. Szymanski, B. Rendy, Y.X. Fei, et al., Nature 624 (2023) 86–91.
[20] Q. Zhu, F. Zhang, Y. Huang, et al., Natl. Sci. Rev. 9 (2022) nwac190.
[21] B. Burger, P.M. Maffettone, V.V. Gusev, et al., Nature 583 (2020) 237–241.
[22] A. Dave, J. Mitchell, S. Burke, et al., Nat. Commun. 13 (2022) 5454.
[23] B.P. Macleod, F.G.L. Parlane, C.C. Rupnow, et al., Nat. Commun. 13 (2022) 995.
[24] B.P. Macleod, F.G.L. Parlane, T.D. Morrissey, et al., Sci. Adv. 6 (2020) eaaz8867.
[25] Y.C. Yin, C. Li, X.S. Hu, et al., ACS Energy Lett. 8 (2023) 3005–3012.
[26] D.X. Zuo, L. Yang, Z.Y. Zou, et al., Adv. Energy Mater. 13 (2023) 2301540.
[27] Y.T. Feng, L. Yang, Z.H. Yan, et al., Energy Storage Mater. 63 (2023) 103053.
[28] W.Y. Liao, F.Z. Qing, Q. Liu, et al., Nano Lett. 25 (2025) 1575–1583.
[29] Y.J. Li, H. Wu, J.F. Zhang, et al., J. Mater. Chem. A 11 (2023) 10267–10276.
[30] C. Li, B.R. Ye, B. Ouyang, et al., Adv. Mater. 37 (2025) 2501381.
[31] X. Yu, Z.Q. Pan, C.G. Pei, et al., Chin. Chem. Lett. 35 (2024) 108484.
[32] J.H. Ma, C.H. Xia, T. Salim, et al., J. Mater. Chem. A 12 (2024) 22597–22608.
[33] C.C. Ye, Z.P. Yu, J. Yang, et al., Angew. Chem. Int. Ed. 137 (2025) e202422451.
[34] W.Y. Zhang, H.X. Jin, Y.N. Guo, et al., Nat. Commun. 16 (2025) 6667.
[35] W. Liu, R.Q. Zhang, C.Y. Li, et al., ACS Catal. 15 (2025) 11886–11895.
[36] G.R. Dey, S. Teklu, Z.X. Shi, et al., J. Am. Chem. Soc. 147 (2025) 24230–24234.
[37] G. Zhang, Y. Gu, L. Li, et al., Chin. Chem. Lett. 36 (2025) 110110.
[38] Z.P. Zhang, S.S. Lu, M.S. Zhu, et al., J. Am. Chem. Soc. 147 (2025) 22806–22817.
[39] X.D. Zhu, W. Huang, Y. Lou, et al., Progress Nat. Sci. Mater. Int. 34 (2024) 880–887.
[40] K. Xiao, Y.F. Wang, P.Y. Wu, L.P. Hou, Z.Q. Liu, Angew. Chem. Int. Ed. 62 (2023) e202301408.